Minority carrier properties of carbon-doped GaInAsN bipolar transistors

2004 J. Phys.: Condens. Matter 16 S3373

(http://iopscience.iop.org/0953-8984/16/31/025)

INSTITUTE OF PHYSICS PUBLISHING JOURNAL OF PHYSICS: CONDENSED MATTER

J. Phys.: Condens. Matter **16** (2004) S3373–S3385 PII: S0953-8984(04)75821-X

Minority carrier properties of carbon-doped GaInAsN bipolar transistors

R E Welser[1], R S Setzko[1], K S Stevens[1], E M Rehder[1], C R Lutz[1], D S Hill[1] and P J Zampardi[2]

[1] Kopin Corporation, 695 Myles Standish Boulevard, Taunton, MA 02780, USA
[2] Skyworks Solutions, 2427 W Hillcrest Drive, Newbury Park, CA 91320, USA

E-mail: rwelser@kopin.com

Received 6 February 2004
Published 23 July 2004
Online at stacks.iop.org/JPhysCM/16/S3373
doi:10.1088/0953-8984/16/31/025

Abstract

We have developed an InGaP/GaInAsN/GaAs double heterojunction bipolar transistor technology that substantially improves upon existing GaAs-based HBTs. Band-gap engineering with dilute nitride GaInAsN alloys is utilized to enhance a variety of key device characteristics, including lower operating voltages, improved temperature stability and increased RF performance. Furthermore, GaInAsN-based HBTs are fully compatible with existing high-volume MOVPE and IC fabrication processes. While poor lifetimes have limited the applicability of dilute nitride materials in photovoltaic applications, we achieve minority carrier characteristics that approach those of conventional GaAs HBTs. We have found that a combination of growth algorithm optimization and compositional grading are critical for improving minority carrier properties in GaInAsN. In this work, we characterize the impact of both carbon and nitrogen doping on minority carrier lifetimes in GaInAsN base layers. Minority carrier lifetimes are extracted from direct measurements on bipolar transistor device structures. Specifically, lifetime is derived from the DC current gain, or β, taken in the bias regime dominated by neutral base recombination. Lifetimes extracted using this technique are observed to be inversely proportional to both carbon and nitrogen doping. As with conventional C-doped GaAs HBTs, current soaking (i.e. burn-in) is found to have a significant impact on GaInAsN HBTs. While we can replicate poor as-grown lifetimes consistent with those reported in photovoltaic dilute nitride materials, our best material to date exhibits nearly 30× higher lifetime after current soaking.

(Some figures in this article are in colour only in the electronic version)

1. Introduction: band-gap engineering the HBT base layer

Integrated circuits employing GaAs-based heterojunction bipolar transistors (HBTs) have developed into a key technology for a variety of commercial and military applications, particularly as power amplifiers (PAs) for wireless handsets. GaAs HBTs offer high linearity and efficiency over a wide frequency range, with high breakdown voltages and single supply voltage operation. Initial implementations of GaAs-based HBTs utilizing either AlGaAs or InGaP alloys for the emitter material have been very successful in the marketplace, with a majority of the wireless phones sold worldwide employing GaAs HBT PAs. Carbon is the preferred dopant in heavily p-type III–V base layers ($\sim 4 \times 10^{19}$ cm^{-3}) because of its low diffusivity [1]. Even higher levels of reliability and improved performance in GaAs-based HBTs can be achieved by replacing AlGaAs with larger energy-gap InGaP as the emitter material [2, 3].

Band-gap engineering of the base layer provides a pathway to fundamentally alter and further enhance the device properties of C-doped InGaP/GaAs HBTs. For instance, the 1.42 eV energy-gap of GaAs results in a notably higher turn-on voltage in GaAs HBTs compared with competing Si and III–V technologies. In the past, lower energy-gap materials lattice matched to GaAs have not been available, significantly constraining GaAs-based HBT technology. Dilute nitride alloys enable the growth of reduced energy-gap material, which can be either lattice matched or strain minimized relative to GaAs. Incorporation of GaInAsN alloys into the base layer of GaAs-based HBTs both lowers the turn-on voltage and enables the implementation of more sophisticated device structures [4]. We have recently reported exciting results from a first-generation technology already in pilot production [5, 6]. At a device level, this graded GaInAsN HBT technology is characterized by a reduction in turn-on, offset and knee voltages, higher speed performance, and improved temperature and bias stability.

While the demonstrated device performance enhancements of bipolar transistors with GaInAsN base layers have been quite significant, we have also observed a degradation in minority carrier lifetime. Such degradation has been commonly reported for dilute nitride materials [7, 8]. In this work, we detail our observations regarding the dependence of minority carrier lifetime in GaInAsN as a function of both carbon and nitrogen doping. We observe that lifetime varies inversely with both carbon and nitrogen concentration, and that it can be increased both by optimization of the growth algorithm and post-growth current soaking. We demonstrate minority carrier properties in GaInAsN (N $\sim$ 0.2%) HBTs that approach those of conventional GaAs HBTs by a combination of improved lifetime and enhanced carrier transport.

2. Carbon doping and the extraction of minority carrier lifetime from HBT structures

The DC current gain, or β, of III–V HBTs is a key device parameter that can be related directly to the minority carrier lifetime and transport properties of the base layer material. Specifically, peak β is typically limited by neutral base recombination in GaAs-based HBTs, and can be estimated by:

$$\beta_{\mathrm{nbr}} \cong v_{\mathrm{b}}\tau / w_{\mathrm{b}} \tag{1}$$

where v_{b} is the average minority carrier velocity across the base, τ is the minority carrier lifetime in the base, and w_{b} is the base thickness [9]. Thus the minority carrier lifetime in C-doped GaAs and GaInAsN can be extracted from direct measurements of β and base thickness in bipolar transistor structures, assuming an average electron velocity across the base layer (appendix A). Figure 1 compares such extracted lifetime versus carbon concentration from

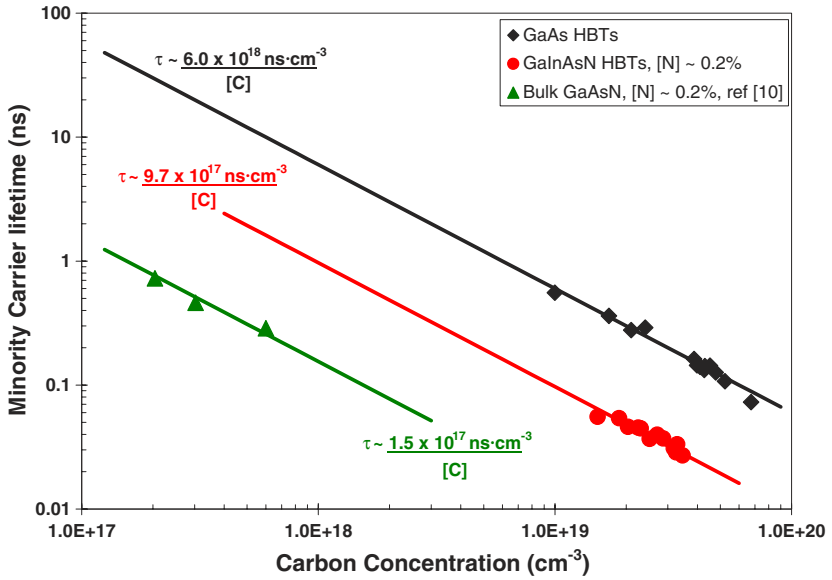

Figure 1. Minority carrier lifetimes as a function of carbon concentration as derived from saturated β (post current soak) in carbon-doped GaAs and GaInAsN ([N] $\sim$ 0.2%) HBTs. For reference, recently reported results for C-doped GaAsN ([N] $\sim$ 0.2%) bulk layers are included [10]. As a guide to the eye, solid lines depict the projected variations of lifetime with carbon concentration for each set of structures.

representative sets of conventional GaAs and GaInAsN HBTs with N $\sim$ 0.2%. Also shown for reference is a published dependence of minority carrier lifetime with carbon concentration in bulk GaAsN layers with similar nitrogen content [10].

All bipolar transistor structures described in this work have MOCVD-grown, C-doped base layers varying between 1–7 $\times$ 10^{19} cm^{-3} in doping and 50–90 nm in thickness, resulting in R_{sb} values between 150 and 1200 $\Omega/\square$. Except for the compositionally graded devices discussed in section 5, all of the GaInAsN structures discussed in this work have constant compositions across the base to simplify the extraction of minority carrier lifetime. InGaP is used as the emitter material to suppress both space charge recombination and reverse hole injection. Large area devices (L = 75 μm $\times$ 75 μm) were fabricated using a simple wet-etching process and tested in the common base configuration as a function of applied base–emitter voltage (V_{be}). Figure 2 shows representative Gummel plots and β characteristics from GaAs and GaInAsN HBTs used in this work. To compute minority carrier lifetime, saturated β values were taken at higher bias where neutral base recombination dominates, as indicated in figure 2(b). Base thickness and doping values were confirmed via cross-sectional scanning electron microscopy and base sheet resistance (R_{sb}) measurements on each individual HBT structure. Hydrogen passivation of the carbon is minimal in these HBT structures ($\sim$0–10%), allowing us to equate carbon concentration [C] with doping level. The nitrogen concentration [N] was estimated based upon a combination of electrical and structural measurements (appendix B).

It is important to note that the β values in figure 2, and hence the computed lifetimes in figure 1, were taken after current stressing to burn in the device, as is common in the industry. Significant increases in β are typically observed in C-doped GaAs HBTs upon initial biasing. In the large area devices discussed here, this increase in β can be unequivocally associated with an increase in base layer minority carrier lifetime. Current densities above 100 A cm^{-2} are required to observe this burn-in phenomenon. The exact mechanism is uncertain, but is clearly

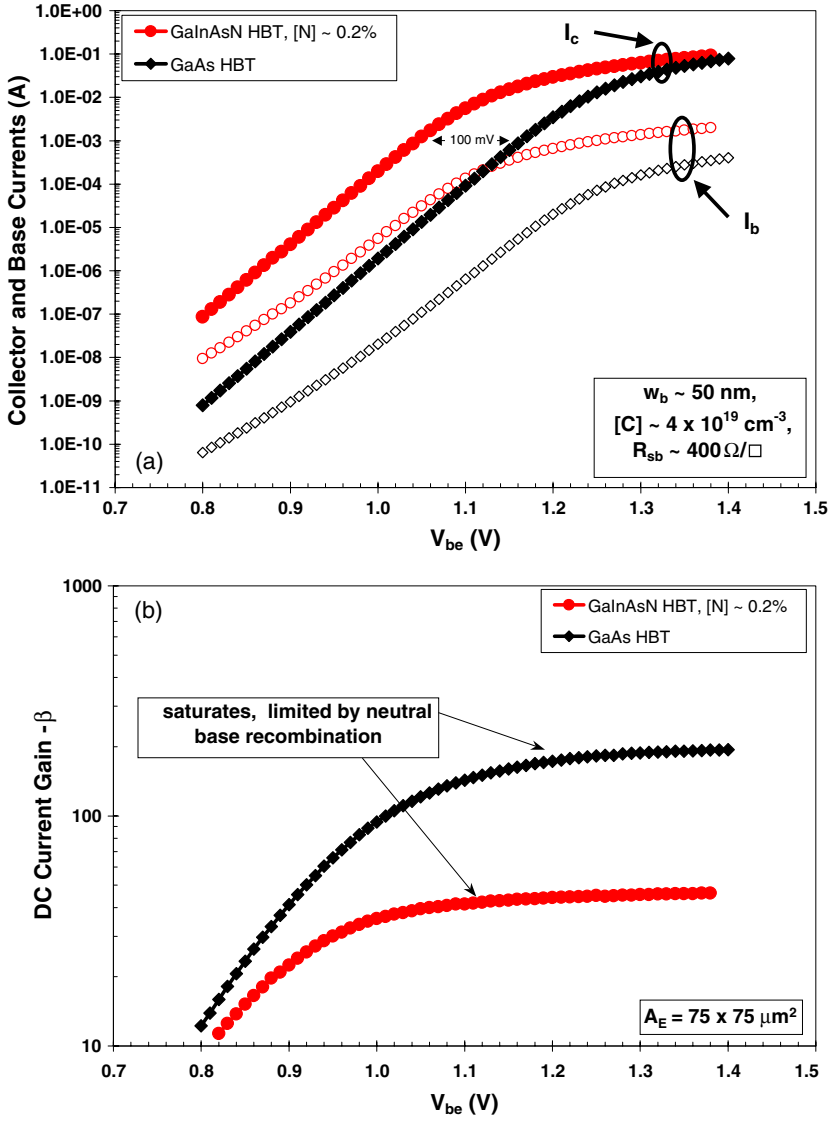

Figure 2. Examples of the (a) Gummel plots and (b) DC current gain, or β, characteristics from GaInAsN ([N] $\sim$ 0.2%) and conventional GaAs HBT structures. The saturated β at $V_{be} > 1.1$ V was used to calculate the minority carrier lifetimes in figure 1.

related to a reduction in trap density or capture rate [11]. The growth conditions employed in the two sample sets of bipolar transistor structures in figure 1 were aimed at minimizing the difference between as-grown and post-current-stress lifetimes (e.g. low burn-in material). This distinction between lifetimes before and after current stressing will be further explored in section 4.

The set of conventional GaAs HBTs used as a benchmark in figure 1 exhibit a gain-to-base-sheet-resistance ratio (β/R_{sb}, a convenient figure of merit) on the order of 0.5, which is indicative of excellent minority carrier properties after current soaking. Indeed, a 60 ns lifetime is projected for [C] $\sim 1 \times 10^{17}$ cm^{-3} material, which is at the high end of the ~20–50 ns often

quoted as the lifetime of high quality p-type GaAs [12]. It is important to note that significant variations in minority carrier lifetime and β with relatively small changes in growth algorithm are common in C-doped GaAs HBTs [9]. The maximum reported β values for 4×10^{19} cm^{-3} GaAs-based HBTs with either AlGaAs or InGaP emitters have steadily increased over the years, with β/R_{sb} exceeding 0.6 in the best cases [9, 13].

The set of GaInAsN HBTs with varying base doping used in figure 1 have approximately 100 mV lower turn-on voltage than the GaAs HBTs, corresponding to a nearly 50× increase in collector saturation current density (figure 2(a)). In all cases the collector current ideality factor (n_c) is near unity, indicating that the effective heights of conduction band spikes at the heterojunctions are minimal. This allows us to equate turn-on voltage reduction to energy-gap difference (appendix B). The nitrogen concentration in this first set of GaInAsN HBTs is minimal ([N] $\sim$ 0.2%, or 4.4×10^{19} cm^{-3}), but comparable to the bulk GaAsN material discussed in [10]. Several additional sets of GaInAsN HBTs with increasing nitrogen concentration will be discussed in subsequent sections.

Perhaps the most striking aspect of figure 1 is that in all three material systems (GaAs, GaAsN, and GaInAsN), minority carrier lifetime varies more or less inversely with carbon concentration. Yet neither radiative nor Auger recombination fundamentally limit the minority carrier lifetime of the materials discussed in this work, given the observed variations in lifetime with both growth algorithm and current stressing. Instead, the inverse dependence with carbon concentration suggests that lifetime is governed by Hall–Shockley–Read processes involving a trap, or traps, proportional to carbon in concentration. While numerous authors have speculated on defects and trap mechanisms in heavily C-doped III–V material, the exact nature of the defects in state-of-the-art material remains largely unknown. Hydrogen-related defects are often associated with the various burn-in phenomena observed in C-doped HBTs [11, 14]. However, hydrogen seems unlikely to limit minority carrier lifetime in material subjected to the appropriate thermal anneals or bias stress. Instead, we suspect that some type of non-hydrogen related defect or defects ultimately limit the lifetime in C-doped HBTs. For instance, Fushimi and Wada have proposed that di-carbon interstitials or As vacancy/carbon acceptor complexes could act as recombination centres in C-doped GaAs [14].

Quantitatively, the lifetime of the C-GaInAsN material with N $\sim$ 0.2% in figure 2 is degraded from typical C-GaAs by $\sim$6×. However, this set of Kopin material is in turn around 6× higher in lifetime than GaAsN with similar N concentration grown for photovoltaic applications. This suggests that N-doping not only degrades lifetime as commonly reported, but that there may be some growth technique dependence.

3. Impact of nitrogen incorporation

The addition of nitrogen to GaInAs is being vigorously pursued for its band-gap and strain-level engineering in quantum-well laser, photovoltaic and bipolar transistor device structures [15–17]. However, the ratios of In and N employed differs for each device application, and results in differing degrees of strain [4]. For photovoltaic applications, lattice-matching is necessary, requiring an In:N ratio $\sim$3. Quantum-well laser structures can withstand large degrees of compressive strain, allowing much larger In-to-N ratios (>20). While the base layers of typical HBTs are thicker than quantum well structures, a fair amount of strain can be still sustained (In:N $\sim$ 15). At Kopin we use nitrogen to maximize the In composition and energy-gap reduction afforded by heavily C-doped InGaAs bases while avoiding film relaxation. In this section, we summarize results from GaInAsN HBTs with increasing levels of nitrogen.

Figure 3 compares Gummel plots from HBTs with GaInAsN and GaAs base layers of comparable doping (2×10^{19} cm^{-3}). Relative to the GaInAsN HBT of figure 2, this sample

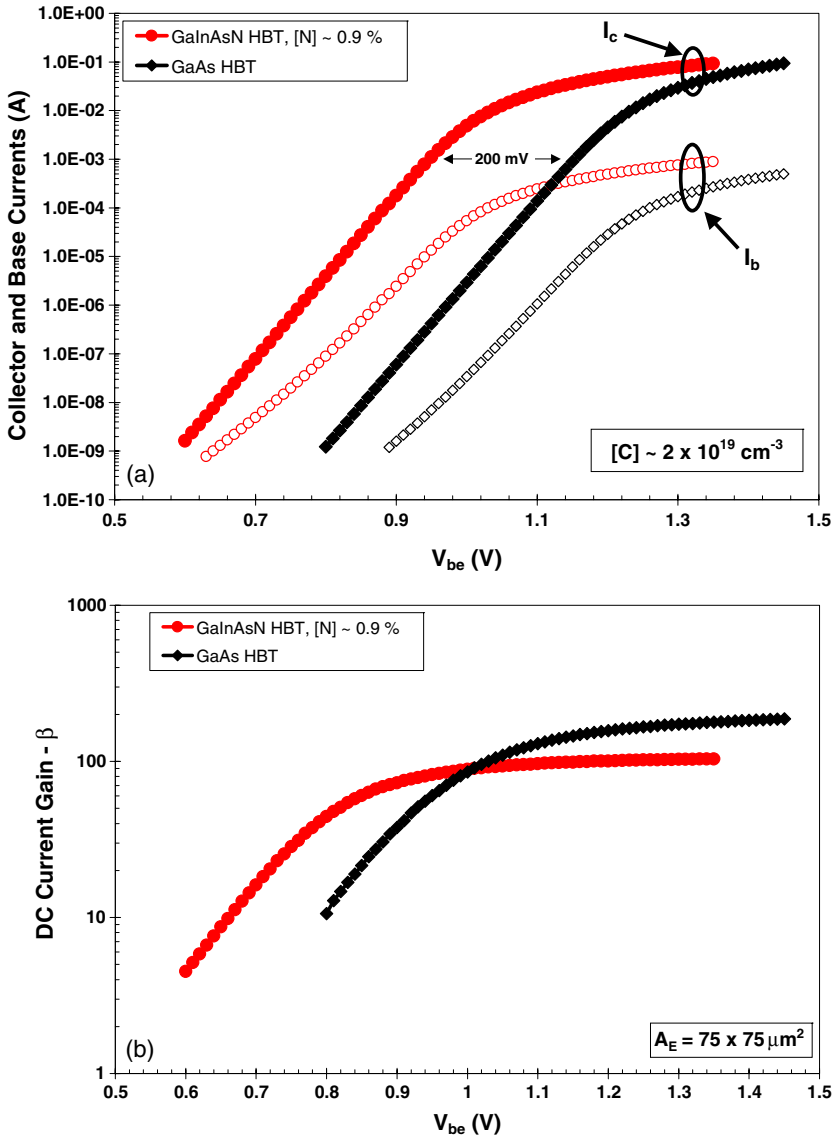

Figure 3. Comparison of the (a) Gummel plots and (b) β versus applied V_{be} from GaInAsN ([N] $\sim$ 0.9%) and conventional GaAs HBT structures with [C] $\sim 2 \times 10^{19}$ cm^{-3}.

has a higher N concentration ($\sim$0.9%), enabling a higher indium content and lower turn-on voltage. Specifically, this GaInAsN base has a 200 mV lower turn-on voltage than the conventional InGaP/GaAs HBT, corresponding to nearly 5000$\times$ higher collector current. The collector current ideality factor is near unity ($n_c \sim 1.018$), again indicating that the effective heights of conduction band spikes at the heterojunctions have been minimized. The DC current gain, or β, is also higher at low bias in this constant composition GaInAsN base ($\beta > 10$ @ $V_{be} = 0.67$ V), and reaches a maximum exceeding 100. To the best of our knowledge, this is the first demonstration of a GaAs-based HBT with 200 mV lower turn-on voltage having $\beta > 100$, and represents a 5$\times$ improvement over previous work [18].

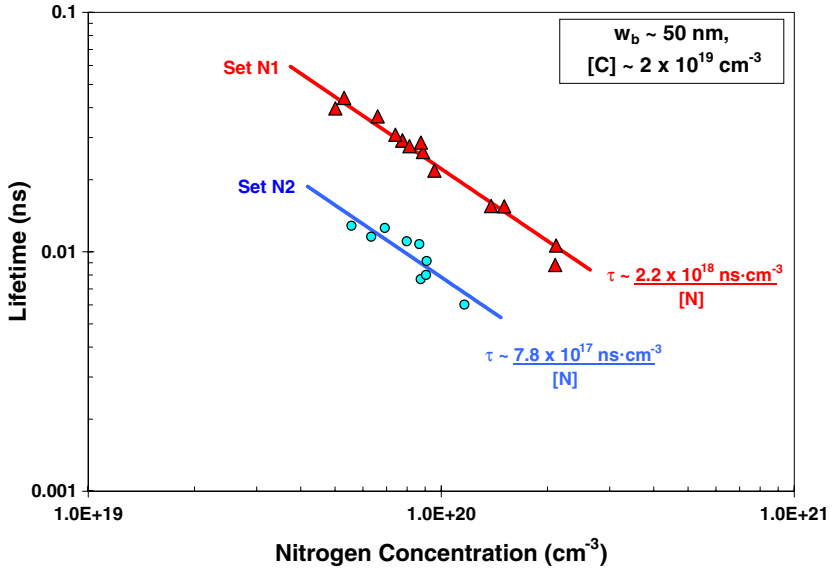

Figure 4. Minority carrier lifetimes as a function of nitrogen concentration as derived from saturated β (post current soak) in two sets of carbon-doped GaInAsN HBTs ([C] $\sim 2 \times 10^{19}$ cm^{-3}). Set N1 is recent work, while set N2 represents typical results from the previous year. As a guide to the eye, solid lines depict the projected variations of lifetime with nitrogen concentration for each set.

Using the C-doped GaInAsN HBT structures discussed previously as a baseline, several subsets of GaInAsN bipolar transistor structures were grown with similar base doping (2×10^{19} cm^{-3}) and N concentrations approaching 1% (set N1). As commonly reported, minority carrier lifetime decreases with nitrogen incorporation, and in this set appears to vary inversely with N concentration (figure 4). Analogous to C-doping, the proportionality between N concentration and lifetime can vary significantly with growth algorithm. For example, our growth optimization efforts have yielded a 3× improvement over the last year (set N1 versus set N2 in figure 4). Compared with C-related defects, even less is known about the nature of N-related defects. However, preliminary studies are beginning to appear in the literature [8].

4. Role of current stress

The data summarized in figures 1 and 4 suggest carbon and nitrogen have a similar impact on the minority carrier lifetime of III–V material. Namely in both cases defects are introduced into the material in a concentration proportional to the carbon and nitrogen levels. Neither radiative nor Auger recombination play limiting roles in the materials discussed here; instead Hall–Shockley–Read trap recombination processes dominate. In this limit the effective minority carrier lifetime (τ) reduces to:

$$\tau \sim \tau_{\mathrm{HSR}([\mathrm{C}],[\mathrm{N}])} \sim \mathrm{CTD}_{\mathrm{HSR}}/[\mathrm{C}]^{\mathrm{Xc}} \quad \text{or} \quad \mathrm{NTD}_{\mathrm{HSR}}/[\mathrm{N}]^{\mathrm{Xn}} \tag{2}$$

where $\tau_{\mathrm{HSR}([\mathrm{C}],[\mathrm{N}])}$ is the Hall–Shockley–Read (HSR) lifetime associated with carbon- and nitrogen-related traps. Also shown is an inverse relation between the trap-dominated lifetime and the carbon- and nitrogen-concentrations, as depicted in figures 1 and 4. The proportionality constants $\mathrm{CTD}_{\mathrm{HSR}}$ and $\mathrm{NTD}_{\mathrm{HSR}}$ relate, among other things, the dopant concentrations to C- and N-related trap densities associated with the HSR processes. In the simplest case the exponents $x_{\mathrm{c}} = x_{\mathrm{n}} = 1$, but are included here for completeness. Note also that our data indicates that

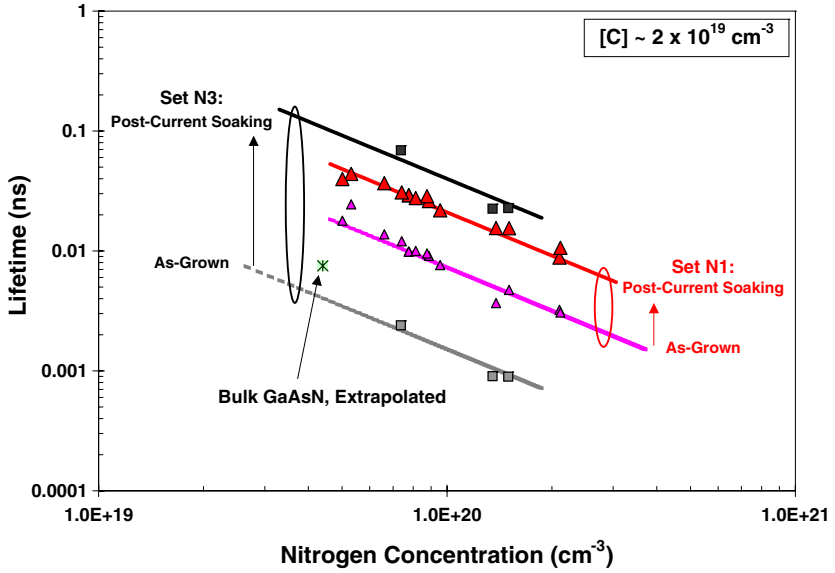

Figure 5. Both as-grown and post-current-soak minority carrier lifetimes as a function of nitrogen concentration in two sets of carbon doped GaInAsN HBTs ([C] $\sim 2\times10^{19}$ cm^{-3}). The post-current-soak minority carrier lifetimes of set N1 were shown previously in figure 4. Set N3 structures were grown using a methodology that results in a nearly 30$\times$ increase in β upon bias. As a guide to the eye, solid (post current soaking) and dashed (as-grown) lines depict the projected variations of lifetime with nitrogen concentration, assuming in this case $x_n = 1.2$. Also shown for reference is the minority carrier lifetime projected for bulk GaAsN with a carbon concentration of 2×10^{19} cm^{-3}, based upon a recent publication [10].

CTD_{HSR} and NTD_{HSR} are not independent, but instead CTD_{HSR} decreases with increasing nitrogen concentration.

As noted previously, we observe that the magnitude of both proportionality constants have definite growth algorithm dependence, suggesting the density of both C- and N-related traps can be minimized with proper optimization. Even so, there is a strikingly large difference between the lifetimes derived from our GaInAsN HBTs with N $\sim$ 0.2% and those of the carbon-doped GaAsN structures of comparable N concentrations described in [10]. While many factors could in principle contribute to this offset (such as material structure, growth chemistry, measurement technique, In concentration, etc), we suggest here that current stressing may play a significant role.

As mentioned in section 2, we observe an increase in β upon current soaking (e.g. burn-in) which results from an increase in the effective minority carrier lifetime in the base layer. This phenomenon is observed in conventional C-doped GaAs HBTs, and can be even more pronounced in C-doped GaInAsN HBTs. The degree of improvement in the post-current-soaking lifetime relative to the as-grown lifetime is sensitive to many aspects of the growth algorithm, including post-growth annealing time and temperature. Under some conditions we observe very large increases ($\sim$30$\times$) in the lifetime of GaInAsN alloys after biasing with currents above 100 A cm^{-2}.

Figure 5 illustrates the dependence of both as-grown and post-current-soaking lifetime as a function of N concentration in two different sets of GaInAsN HBTs. Set N1 has been discussed previously, and exhibits a moderate change in lifetime upon current soaking. Set N3 has been grown using an algorithm aimed at maximizing only post-current-soaking β (and lifetime),

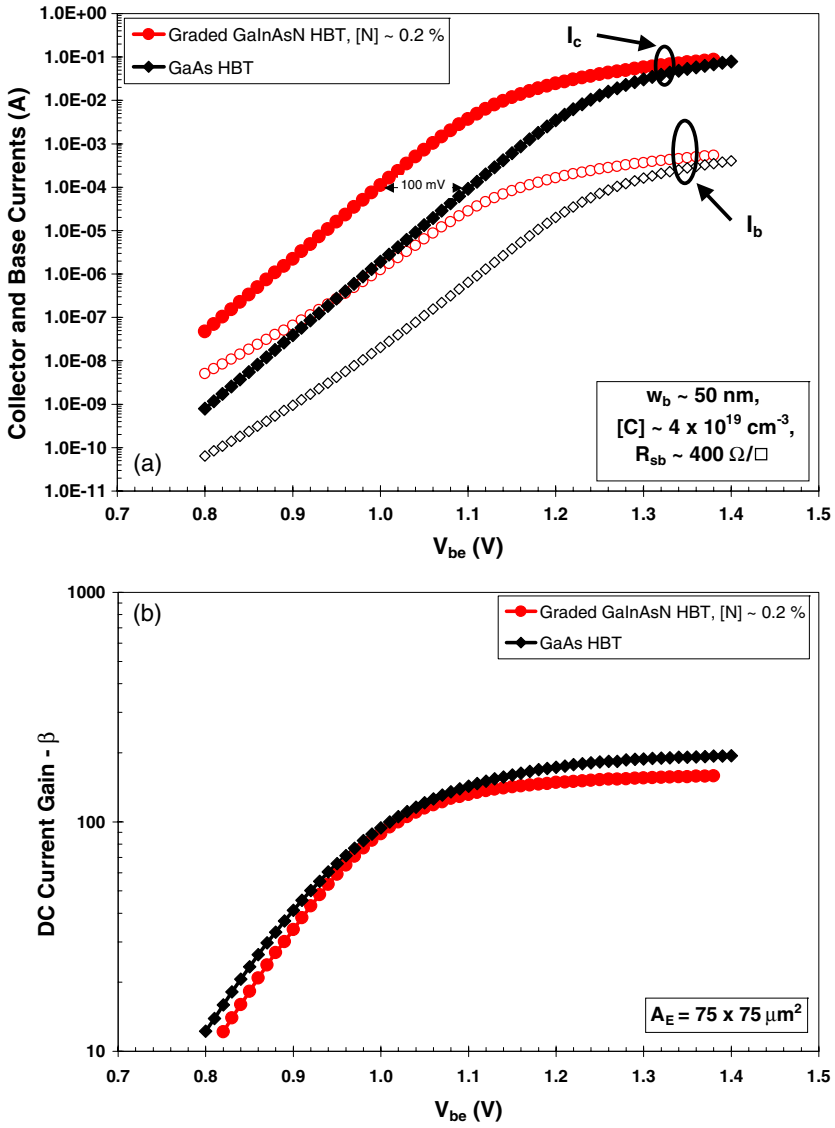

Figure 6. (a) Gummel plots and (b) β versus applied V_{be} from graded GaInAsN ([N] $\sim$ 0.2%) base and conventional GaAs HBT structures with similar base thickness, doping and sheet resistance values.

and exhibits a large degree of burn-in ($\sim$30$\times$). Note that the as-grown lifetimes of the material in set N3 nearly matches that expected from the GaAsN material described by Kurtz *et al* [10] when extrapolated to [C] $\sim 2\times10^{19}$ cm^{-3}. However, this lifetime is over an order of magnitude lower than our best post-current-soaking lifetimes at similar N and C concentrations.

5. Enhancing minority carrier properties with compositionally graded structures

We have achieved minority carrier characteristics with dilute nitrides that approach conventional GaAs HBTs. This has been accomplished by a combination of improved minority carrier lifetime and the implementation of compositionally graded base structures. As shown

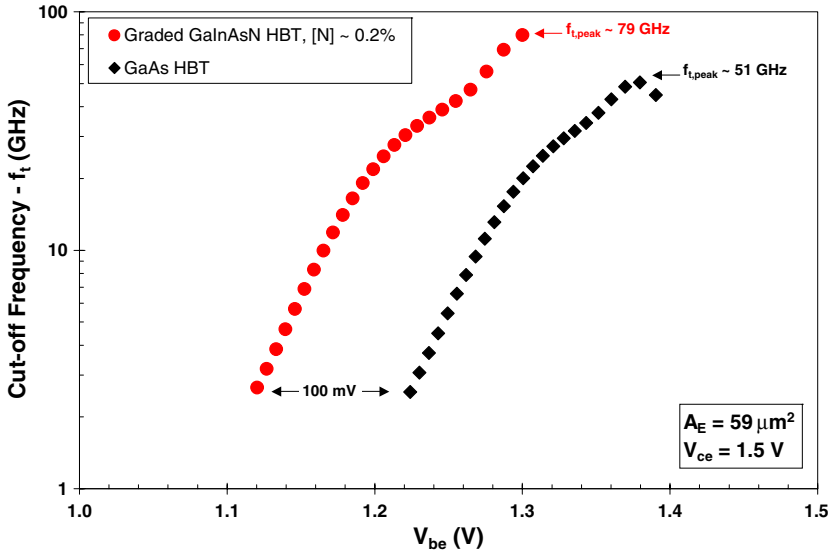

Figure 7. Maximum cut-off frequency (f_t) versus applied V_{be} from graded GaInAsN ([N] $\sim$ 0.2%) base and conventional GaAs HBT structures with comparable collector structures ($BV_{ceo} \sim$ 12.5 and 14.5 V, respectively).

in this work, the minority carrier lifetime of dilute nitrides can be increased by both growth optimization and post-growth current stressing. The DC current gain of GaAs-based HBTs can also be maximized by increasing the average carrier velocity (see equation (1)). We have previously demonstrated that built-in drift fields resulting from compositional grading of the GaInAsN base layer is an effective means of enhancing base transport [4, 5, 19]. Figure 6 compares the Gummel plot characteristics of a graded GaInAsN base ([N] $\sim$ 0.2%) to those of a conventional GaAs HBT of similar base thickness, doping and sheet resistance. Relative to the conventional GaAs HBT, the graded GaInAsN HBT has a 100 mV lower turn-on voltage. In both cases the collector current ideality factor (n_c) is near unity, a key requirement for ideal HBT operation. The DC current gain of the graded GaInAsN base reaches a maximum (β_{max}) of greater than 150. While the β_{max} of the GaInAsN device is slightly lower than that of state-of-the-art InGaP/GaAs HBTs ($\beta_{max} \sim 200$ @ 400 $\Omega/\square$), this GaInAsN HBT exhibits a $\beta/R_{sb} \sim 0.35$, approaching that of many GaAs HBTs in production. To the best of our knowledge, this is the highest gain-to-base-sheet reported for any GaAs-based HBT with a 100 mV turn-on reduction.

The higher average electron velocity resulting from built-in fields also enhances the RF properties of graded GaInAsN devices. As an example, figure 7 compares the maximum frequency of operation (f_t) of a graded GaInAsN HBT to that of a conventional GaAs HBT. The lower average base energy-gap of the graded GaInAsN structure results in a 100 mV shift in the f_t characteristics. The lower base transit time results in a significant increase in the maximum f_t, from 51 to 79 GHz. Additional device level benefits of the graded GaInAsN HBT structure have been reported elsewhere [5, 6].

6. Conclusions

Band-gap engineering with dilute nitride GaInAsN alloys provides a promising pathway for enhancing key device characteristics in GaAs-based HBTs. The minority carrier lifetime, a critical parameter impacting HBT device parameters, has been extracted directly from bipolar

transistor structures via measurements of the saturated DC current gain in large area devices. Lifetime is observed to decrease with increasing carbon and nitrogen levels, consistent with the introduction of Hall–Shockley–Read-type defects along with the C and N dopants. The proportionality between trap density and carbon or nitrogen levels is found to vary by several orders of magnitude depending on growth algorithm and current soaking. The nature of these defects is far from understood. Nevertheless, excellent minority carrier properties are achieved in GaInAsN HBT structures employing built-in electrical fields and grown under optimized conditions.

Acknowledgments

The authors would like to thank the efforts and support of the entire GaAs Transistor Group at the Kopin Corporation, particularly the material characterization efforts of V Un, S Lawlor and M Brooks, the engineering support of R McCullough and E Brown, as well as fruitful discussions with P M DeLuca, B E Landini, and M Micci.

Appendix A. Average electron velocity

Extraction of the base layer minority carrier lifetime directly from measurements on bipolar transistor structures requires the confirmation of a number of critical assumptions. First and foremost, the β value must be taken in a regime in which neutral base recombination dominates, and for which equation (1) is thus valid. In this work we have used large area devices in which surface recombination around the device perimeter can be reasonably ignored. Intrinsic space charge recombination, with an $n = 2$ ideality factor, is avoided by taking the β at high bias. Furthermore, reverse hole injection is negligible at room temperature in GaAs HBTs with InGaP emitters. Fits of the collector and base current components confirm the dominance of neutral base recombination [9]. Even so, we acknowledge that the precision of this method for extracting carrier lifetime is compromised by ∼10 to 20%, in that β typically continues to increase slowly with bias in GaAs-based HBTs, even when neutral base recombination is clearly the limiting mechanism. The exact cause of this observed increase in β is still under investigation.

Once the saturated neutral recombination β is measured, accurate estimates of the average electron velocity must be made before deriving lifetime. Base transit time, and hence average electron velocity, is often assumed to obey a simple diffusive mechanism (i.e. with infinite exit velocity). However, experimental data clearly indicates more complex mechanisms are necessary to account for electron transport across the base of GaAs HBTs [20]. While quasiballistic transport models may provide the most accurate description of GaAs HBT characteristics, we can also quite reasonably describe experimental data with a finite exit velocity approximation, assuming a proper choice of diffusion coefficient (D_n) and exit velocity (v_{exit}). In this limit, the average electron velocity across the base is:

$$v_b = v_{exit}/(1 + w_b v_{exit}/2D_n). \tag{3}$$

In this work we assume the exit velocity is limited by the field across the base–collector junction, and arrive at a value of 9×10^6 cm s^{-1} [21]. We have assumed that the diffusion coefficient varies with doping in a manner similar to the theory of Lowney and Bennet, but shifted upward to match more recent experimental data ($D_n = 90.5$ cm^2 s^{-1} @ 4×10^{19} cm^{-3}) [22, 23]. Equation (3) with $v_{exit} = 9 \times 10^6$ cm s^{-1} and $D_n \sim 90.5$ cm^2 s^{-1} yields a nearly constant v_b for base thickness in the 50–90 nm range, which is in turn consistent with the near linear variation of β with R_{sb} typically observed in GaAs HBTs [9]. While these choices of exit velocity

and diffusion coefficient predict longer base transit times than often assumed (e.g. [24]), the projected values are no higher than published estimates in [25]. The above choice of D_n and v_{exit} is also consistent with collector current transport data, both from Kopin and other laboratories [20, 26].

In this work we have assumed D_n and v_{exit} to be independent of base material composition. This may be reasonable for v_{exit} if it is ultimately limited by transport in the GaAs collector. On the other hand, the diffusion constant D_n may be expected to decrease in the quaternary alloys, which would then cause us to underestimate the minority carrier lifetimes of GaInAsN. However, we have observed excellent maximum cutoff frequency performance in GaInAsN HBTs (figure 7) [5, 6], suggesting the degradation in D_n, if any, must be minimal.

Appendix B. Estimation of nitrogen concentration

The nitrogen concentration is estimated from measurements made directly on the bipolar transistor structure. First the energy gap reduction is determined by comparing the GaInAsN transistor turn-on voltage to that of GaAs bipolar transistors of identical base sheet resistance (e.g. [26]). In the limit of $n_c \sim 1$, this turn-on voltage difference (ΔV_{be}) can be equated to an energy-gap difference ($\Delta E_g = E_{gGaInAsN} - E_{gGaAs}$). The peak splitting of the pseudomorphic GaInAsN base layer relative to the GaAs substrate is measured via standard double-crystal x-ray diffraction. Experimental data from a set of heavily doped GaInAs ($N = 0\%$) bipolar transistors is used to separate out the role of In on energy-gap and x-ray splitting. The percentage of nitrogen is then estimated assuming literature values for the impact of nitrogen on x-ray splitting and energy-gap [10, 27]. We note that in quantifying the relative value of the alloy energy-gap, rather than the absolute value, we avoid the need to quantify the complicating effects of band-gap narrowing and compressive strain, phenomena which are not yet well characterized in the dilute nitrides.

References

[1] Wang G-W, Pierson R L, Asbeck P M, Wang K-C, Wang N-L, Nubling R, Chang M F, Shastry S K, Hill D S and Salerno J P 1991 High-performance MOCVD-grown AlGaAs/GaAs heterojunction bipolar transistors with carbon-doped base *IEEE Electron Devices Lett.* **12** 347–9

[2] Low T, Shirley T, Hutchinson C, Ossified G, Whitely W, Yeast B and D'Avanzo D 1999 InGaP HBT technology for RF microwave instrumentation *Solid-State Electron.* **43** 1437–44

[3] Welser R E, Pan N, Lutz C R, Vu D P, Zampardi P J, Pierson R L and McDermott B T 2000 High performance $Al_{0.35}Ga_{0.65}As$/GaAs HBT's *IEEE Electron Devices Lett.* **21** 196–9

[4] Asbeck P M, Welty R J, Tu C W, Xin H P and Welser R E 2002 Heterojunction bipolar transistors implemented with GaInNAs materials *Semicond. Sci. Technol.* **17** 898–906

[5] DeLuca P M, Lutz C R, Welser R E, Chi T Y, Huang E K, Welty R J and Asbeck P M 2002 Implementation of reduced turn-on voltage InGaP HBTs using graded GaInAsN base regions *IEEE Electron Devices Lett.* **23** 582–4

[6] Yarborough R, Landini B, Welser R, Yang J and Henderson T 2002 Enhanced CDMA performance from an InGaP/GaInAsN/GaAs N–p–N double heterojunction bipolar transistor *2002 IEEE GaAs IC Symp. Technical Digest* pp 273–6

[7] Geisz J F and Friedman D J 2002 III-N-V semiconductors for solar photovoltaic applications *Semicond. Sci. Technol.* **17** 769–77

[8] Janotti A, Wei S-H, Zang S B, Kurtz S and Van de Walle C G 2003 Interactions between nitrogen, hydrogen, and gallium vacancies in $GaAs_{1-x}N_x$ alloys *Phys. Rev.* B **67** 161201

[9] Welser R E, Pan N, Vu D P, Zampardi P J and McDermott B T 1999 Role of neutral base recombination in high gain AlGaAs/GaAs HBTs *IEEE Trans. Electron Devices* **46** 1599–607

[10] Kurtz S R, Geisz J G, Keyes B M, Metzger W K, Friedman D J, Olson J M, King R R and Karam N H 2003 Effect of growth rate and gallium source on GaAsN *Appl. Phys. Lett.* **82** 2634–6

[11] Henderson T, Ley V, Kim T, Moise T and Hill D 1996 Hydrogen-related burn-in in GaAs/AlGaAs HBTs and implications for reliability *Proc. IEDM* pp 203–6
[12] Nelson R J and Sobers R G 1978 Minority-carrier lifetimes and internal quantum efficiency of surface-free GaAs *J. Appl. Phys.* **49** 6103–8
[13] Chung T, Bank S and Hsieh K C 2000 High DC current gain InGaP/GaAs HBTs grown by LP-MOCVD *Electron. Lett.* **36** 1885–86
[14] Fushimi H and Wada K 1997 Carbon-related defects in carbon-doped GaAs by high-temperature annealing *J. Appl. Phys.* **82** 1208–13
[15] Nakahara K, Kondow K, Kitatani T, Yazawa Y and Uomi K 1996 Continuous-wave operation of long-wavelength GaInNAs/GaAs quantum well laser *Electron. Lett.* **32** 1585–86
[16] Kurtz S R, Allerman A A, Jones E D, Gee J M, Banas J J and Hammons B E 1999 InGaAsN solar cells with 1.0 eV band gap, lattice matched to GaAs *Appl. Phys. Lett.* **74** 729–31
[17] Welty R J, Xin H, Tu C W and Asbeck P M 2004 Minority carrier transport properties of GaInNAs heterojunction bipolar transistors with 2% nitrogen *J. Appl. Phys.* **95** 327–33
[18] Monier C, Baca A G, Chang P C, Newman F D, Li N Y, Sun S Z, Armour E and Hou H Q 2002 Significant operating voltage reduction on high-speed GaAs heterojunction bipolar transistors using a low band gap InGaAsN base layer *IEEE Trans. Electron Devices* **49** 1329–35
[19] Stevens K S, Welty R J, Welser R E, Landini B E, Asbeck P M, Hung S-C, Lu W-P and Feng S-C 2004 Impact of compositionally graded base regions on the DC and RF properties of reduced turn-on voltage InGaP/GaInAsN DHBTs *IEEE Trans. Electron Devices* submitted
[20] Harmon E S, Melloch M R, Lundstom M S and Cardone F 1994 Thermal velocity limits to diffusive electron transport in thin-base $np^{+}n$ GaAs bipolar transistors *Appl. Phys. Lett.* **64** 205–7
[21] Toorn R V, Paasschens J C J and Havens R J 2003 A physically based analytical model of the collector charge of III–V heterojunction bipolar transistors *2003 IEEE GaAs IC Symp. Technical Digest* pp 111–4
[22] Lowney J R and Bennett H S 1991 Majority and minority electron and hole mobilities in heavily doped GaAs *J. Appl. Phys.* **69** 7102–10
[23] D'Souza S L, Melloch M R, Lundstom M S and Harmon E S 1997 Technique for measurement of the minority carrier mobility with a bipolar junction transistor *Appl. Phys. Lett.* **70** 475–7
[24] Maziar C M and Lundstom M S 1987 On the estimation of base transit time in AlGaAs/GaAs bipolar transistors *IEEE Electron Devices Lett.* **8** 90–2
[25] Ahmari D A, Fresina M T, Hartman Q J, Barlage D W, Mares P J, Feng M and Stillman G E 1996 High-speed InGaP/GaAs HBT's with a strained $In_xGa_{1-x}As$ base *IEEE Electron Devices Lett.* **17** 226–28
[26] Welser R E, DeLuca P M and Pan N 2000 Turn-on voltage investigation of GaAs-based bipolar transistors with $Ga_{1-x}In_xAs_{1-y}N_y$ base layers *IEEE Electron Devices Lett.* **21** 554–6
[27] Bellaiche L, Wei S-H and Zunger A 1997 Band gaps of GaPN and GaAsN alloys *Appl. Phys. Lett.* **70** 3558–60